0026-895X/06/6901-130–139$20.00
MOLECULAR PHARMACOLOGY
Copyright © 2006 The American Society for Pharmacology and Experimental Therapeutics
Mol Pharmacol 69:130–139, 2006

Vol. 69, No. 1
15933/3074634
Printed in U.S.A.

Mutation P732L in Human DNA Topoisomerase IIβ Abolishes DNA Cleavage in the Presence of Calcium and Confers Drug Resistance

Chrysoula Leontiou,[1] Jeremy H. Lakey, Robert Lightowlers, Rozalind M. Turnbull, and Caroline A. Austin

Institute for Cell and Molecular Biosciences, The Medical School, University of Newcastle upon Tyne, United Kingdom

Received June 21, 2005; accepted October 20, 2005

ABSTRACT

The anti cancer drug methyl *N*-(4′-(9-acridinylamino)-3-methoxy-phenyl) methane sulfonamide (mAMSA) targets human DNA topoisomerase IIβ. We report here the first selection with mAMSA of resistant human topoisomerase IIβ. Random mutagenesis of human DNA topoisomerase IIβ cDNA, followed by selection in yeast for resistance to mAMSA, identified βP732L. This mutant was 10-fold less sensitive to mAMSA and cross-resistant to other chemotherapeutic agents such as etoposide, ellipticine, methyl *N*-(4′-(9-acridinylamino)-2-methoxy-phenyl) carbamate hydrochloride (mAMCA), methyl *N*-(4′-(9-acridinylamino)-phenyl) carbamate hydrochloride (AMCA), and doxorubicin. βP732L is functional but has reduced strand passage activities and altered DNA binding compared with the wild-type protein. It has drastically altered cleavage properties compared with the wild-type enzyme. It cleaved a 40-base pair (bp) DNA substrate in the presence of magnesium but at positions different from that of the wild-type protein. More striking is that βP732L was unable to cleave the 40-bp DNA substrate, a 500-bp linear substrate, or a 4.3-kilobase supercoiled substrate in the presence of calcium ions. This is the first report of a topoisomerase II mutation abolishing the ability of calcium to support DNA cleavage. This provides evidence for metal ion requirement for the phosphoryltransfer reaction of topoisomerase II and a possible mechanism for drug resistance.

Topoisomerases regulate DNA topology. For example, during replication and transcription, positive and negative supercoils are generated and topoisomerases are necessary to regulate the degree of supercoiling generated by these processes. Topoisomerase II activity is essential for segregation of chromosomes during cell division and for maintaining chromosome structure during mitosis. As indispensable enzymes for cell cycle progression, topoisomerases are a good target for chemotherapeutic drugs used in cancer therapy. Type II DNA topoisomerases (topo II) catalyze topological changes in DNA by passing a double helix through another in a reaction coupled to ATP hydrolysis. The mechanism of action of topo II enzymes involves cleavage of double-stranded DNA followed by passage of a second duplex and religation of the cleaved DNA duplex (Wang, 2002).

Humans have two topo II isoforms, termed α and β. We have shown that both human topo II isoforms are poisoned by the anticancer drug mAMSA both in vitro and in vivo and that they had similar DNA cleavage site determinants in the presence of this cytotoxic drug (Marsh et al., 1996; Meczes et al., 1997). mAMSA increases the formation of DNA cleavage sites by inhibiting the religation reaction (Robinson et al., 1991). Further evidence that mAMSA can target both isoforms has come from studies with a pair of murine embryo fibroblast cell lines with and without topo IIβ (Errington et al., 1999). In another study, in which topo IIβ was transfected back into cells lacking topo IIβ, restoration of sensitivity to amsacrine (mAMSA) was seen, confirming topo IIβ as a target of mAMSA (Dereuddre et al., 1997).

All topo II poisons stabilize the normally transient cleavage intermediates or cleavable complexes; this DNA damage triggers apoptosis (Tewey et al., 1984; Pommier et al., 1991). Mutations in topo II genes that impair the ability of the drug to bind to the enzyme or decrease the DNA binding and cleavage properties of topo II enzymes can cause drug resistance (Pommier, 1993).

This work was supported by Cancer Research UK (C.L.) and The Wellcome Trust.

[1] Current affiliation: ETH Zürich, Institute for Molecular Biology and Biophysics, ETH-Hoenggerberg, Zürich, Switzerland.

Article, publication date, and citation information can be found at http://molpharm.aspetjournals.org.
doi:10.1124/mol.105.015933.

ABBREVIATIONS: topo, DNA topoisomerase; mAMSA, amsacrine [methyl *N*-(4′-(9-acridinylamino)-3-methoxy-phenyl) methane sulfonamide]; AMCA, methyl *N*-(4′-(9-acridinylamino)-phenyl) carbamate hydrochloride; mAMCA, methyl *N*-(4′-(9-acridinylamino)-2-methoxy-phenyl) carbamate hydrochloride; kDNA, kinetoplast DNA; htopo, human DNA topoisomerase; MLC, minimum lethal concentration; bp, base pair(s); βwt, β wild type.

Several model systems have been used to select mAMSA drug resistance mutations in topo II to elucidate how this drug interacts with its target. Two mutations in the genes encoding bacteriophage T4 topo II have been reported to give rise to mAMSA-resistant T4 (Freudenreich et al., 1998). The yeast model system uses a strain bearing a temperature-sensitive topo II that can be rescued at the nonpermissive temperature by a plasmid-borne functional topo II. This system has been used to select mAMSA-resistant mutations in both yeast topo II and human topo IIα. Mutations at two positions in yeast topo II were identified, K478A (within the conserved PLRG***K*** motif) and A642G (Wasserman and Wang, 1994). Use of this system also identified two mutations in human topo IIα, R486K and E571K, that conferred resistance to mAMSA. Arg486 is in the conserved PL***R***GK motif (Patel et al., 2000). (The bold, italic letter shows the position of the mutated amino acid residue.) In addition, several human cell lines that are resistant to mAMSA have been shown to bear a point mutation R486K in human topoisomerase IIα (Bakic et al., 1986; Hinds et al., 1991; Lee et al., 1992; Kubo et al., 1996)

In this article, we report the first use of the yeast model system to select for mAMSA resistance in human topo IIβ. Randomly mutagenized plasmids encoding human topo IIβ were transformed into a *Saccharomyces cerevisiae* strain and grown in the presence of mAMSA. htopo IIβ bearing a P732L mutation was selected. In vitro characterization of P732L revealed that this mutation had distinct cleavage properties compared with the wild type. To our knowledge, it is the first mutation in a type II topoisomerase that is able to cleave DNA in the presence of magnesium ions but not calcium ions.

Materials and Methods

Reagents

Chemicals and Drugs. mAMSA was obtained from the National Cancer Institute (Bethesda, MD). AMCA and mAMCA were supplied by Prof. B. C. Baguley (Auckland Cancer Society Research Center, University of Auckland, Auckland, New Zealand). Etoposide, mitoxantrone, doxorubicin, and ellipticine were purchased from Sigma (St. Louis, MO). DNA sequencing was carried out by Lark Technologies Inc (Essex, UK). Oligonucleotides were ordered from Invitrogen (Paisley, UK). Radiochemicals were purchased from GE Healthcare (Little Chalfont, Buckinghamshire, UK) and enzymes from New England Biolabs (Hertfordshire, UK) or Promega (Southampton, UK). kDNA was purchased from TopoGEN, Inc. (Port Orange, FL).

Yeast Strains and Expression Plasmids.

- JN394t2–4: *α ISE2 urs3–52 top2-4 rad52::LEU2*. A yeast strain carrying a temperature sensitive mutation in the yeast topoisomerase II gene that makes yeast viable at 25°C but nonviable at 35°C (Nitiss, 1994).
- *JEL1Δtop1*: A protease-deficient *S. cerevisiae* strain for the expression of topo II: *α leu2 trp1 ura3–52 prb1–1122pep4–3 Δhis3::PGAL4*.
- *YEphTOP2βKLM*: carries the first five codons of the *TOP2* gene fused to codons 46 to 1621 of the human TOP2β cDNA (βwt) (Meczes et al., 1997).

Hydroxylamine Mutagenesis and Selection in the Presence of mAMSA. Random mutagenesis and selection for drug resistance was as described previously (Leontiou et al., 2004), except that the selecting agent was mAMSA at 190 μM (74.7 μg/ml), twenty times the IC_{50} value in yeast (Meczes et al., 1997). The wild-type htopo IIβ (βwt) cDNA was mutagenized by exposure to hydroxylamine. This library of randomly mutated plasmids was then transformed into the yeast strain JN394 top2-4 in which growth at the nonpermissive temperature is dependent upon a functional plasmid-borne topo II. Drug-resistant transformants were selected by exposure to 190 μM (75 μg/ml) mAMSA in liquid culture for 96 h. The surviving yeast were plated on drug-free plates and grown for 5 to 7 days at 35°C; approximately 500 colonies grew. Of these, 36 were resistant when re-streaked onto plates containing mAMSA. Plasmids were rescued from these resistant yeast transformants. Yeast strain JN394 top2-4 was retransformed with these plasmids, and the transformants were grown on plates containing mAMSA to confirm whether their drug resistance was plasmid-borne. After retransformation, only three of the 36 grew on plates containing 10 μg/ml mAMSA, so only these three had plasmid-borne resistance. To confirm that a single point mutation in YEphTOP2βKLM was the cause of the drug resistance phenotype, a fragment exchange was performed (Leontiou et al., 2004). Fragment exchange of the 1674-bp region that contained the C-to-T change, resulting in the βP732L mutation into an unmutagenized vector, was performed. The fragment-exchanged construct was transformed into the JN394 top2-4 strain. The temperature sensitive mutation in the endogenous topo II gene in this strain permits growth of the yeast cells at 25°C but not 35°C.

Drug sensitivity was determined via the minimum lethal concentration (MLC), after short-term exposure to mAMSA in liquid culture or by continuous drug exposure by plating the yeast on agar plates containing drugs at a range of concentrations and incubation at 35°C for 3 to 5 days (Leontiou et al., 2004).

Protein Expression and Purification

Recombinant htopo IIβ proteins were expressed in the yeast strain JEL1Δtop1 bearing plasmid YEphTOP2βKLM or YEphTOP2βP732L. Recombinant proteins were produced as described previously (Austin et al., 1995).

Strand Passage Assays

Decatenation and relaxation assays were carried out in relaxation buffer (50 mM Tris-HCl, pH 7.5, 0.5 mM EDTA, 1 mM dithiothreitol, 100 mM KCl, and 30 μg/ml bovine serum albumin) with 1 μg of supercoiled pBR322 plasmid DNA or 400 ng of kinetoplast DNA, 2 mM ATP, and 10 mM $MgCl_2$, as described previously (Austin et al., 1995).

DNA Cleavage Assays

The cleavage properties of βwt and βP732L proteins were tested by incubating the protein with a ^{32}P-end labeled 40-bp linear DNA substrate. The cleavage religation equilibria of βwt and βP732L were tested in the presence of 10 mM $MgCl_2$ or $CaCl_2$ to test the non–drug-stimulated cleavage properties of the enzymes and in the presence of mAMSA (10 μg/ml) to compare the drug-stimulated cleavage of βwt and βP732L (Osheroff and Zechiedrich, 1987). To calculate the relative cleavage under these conditions, the amount of end-labeled cleaved product in several experiments was quantified using filmless autoradiographic analysis using a Fujifilm BAS-1500 machine. The amount of cleavage with wild-type protein in the presence of mAMSA and magnesium was taken as 100%, and the cleavage under different conditions was calculated relative to this (Marsh et al., 1996).

Cleavage was also analyzed on a 564-bp end-labeled fragment, on 4.3-kilobase linearized pBR322, and on supercoiled plasmid DNA. In all of the cleavage experiments, the protein was in excess over the DNA. For example, in the 40-bp cleavage experiments, there was a 10-fold molar excess of protein over DNA (3 and 0.3 pmol, respectively), whereas in the supercoiled cleavage, there was only a 2-fold molar excess of protein over DNA (1 and 0.5 pmol, respectively).

Reversal of Cleavage Assays

A 564-bp fragment of pBR322 was amplified by polymerase chain reaction, and reversibility experiments were carried out as described in (Leontiou et al., 2004).

Surface Plasmon Resonance

The DNA binding properties of the βwt and βP732L proteins were tested by surface plasmon resonance on a BIAcore 2000 (BIAcore AB, Uppsala, Sweden). The DNA substrates used were a 40-bp linear oligonucleotide (the same substrate used for the cleavage assays), a synthetic four-way junction substrate, and a piece of bent DNA from the *Drosophila melanogaster* genome. The linear 40-bp substrate contains a single mAMSA cleavage site and allows the binding of one topo II dimer. The 4wj substrate contains the sequence of the 40-bp linear substrate along two adjacent arms, with the cleavage site straddling the point of strand exchange. The bent DNA substrate is a 189-bp AT-rich region from the *D. melanogaster* genome that forms a bend.

Topo II-DNA binding was carried out in 50 mM Tris-HCl, pH 7.7, 1 mM EDTA, 1 mM EGTA, 100 mM KCl, 1 mM ATP, 0.05% (v/v) Tween p20, and 1% (v/v) Triton X-100. Protein samples were injected using the BIAcore function 'kinject' at a flow rate of 70 μl/min. The protein was injected for 60 s, and the dissociation phase was recorded for 180 s at 25°C. After injection, the chip was regenerated by a 30-s pulse of 0.5% (w/v) SDS followed by a 60-s injection of 0.5 M NaCl. The concentration range of protein used was 5 to 60 nM. When protein becomes bound to DNA on the sensor chip, the refractive index of the medium at the chip surface is affected. This alteration is referred to as a change in RU, which represents an indirect measure of the amount of bound protein.

The association and dissociation data were modeled and analyzed by using BIAevaluation software, version 3.0 (BIAcore). The association and dissociation phases were analyzed for several protein concentrations. Data were fitted by using the numerical integration method. The residual plots and the χ^2 values were used to assess the appropriateness of the various models available for analyzing the sensor data. In general, values of $\chi^2 < 10$ were accepted.

Topo II DNA binding data were produced for various protein concentrations and were fitted simultaneously, assuming the 1:1 Langmuir model. The Langmuir model assumes that the analyte is both monovalent and homogeneous, that the ligand is also homogeneous, and that binding events are independent. The binding of topo II to DNA follows first-order kinetics: A + B ↔ AB. The fitting parameters provide estimates of both association and dissociation rate constants (k_a and k_d), and from these values, the equilibrium constants K_A and K_D were calculated ($K_D = k_d/k_a$ and $K_A = k_a/k_d$) (Leontiou et al., 2003).

Protein Structure Analysis. Protein structures were manipulated and displayed using QUANTA, release 4.1.1. (Accelrys, San Diego, CA) on an SGI workstation (Mountain View, CA). Human DNA topoisomerase IIβ was modeled on the yeast crystal structure using the program Modeler (Sali and Blundell, 1993), as described by West et al. (2000). The structure was used to model the effect of the proline-to-leucine mutation at position 732. The model was subjected to an energy minimization cycle using Charmm (50 steps steepest descents). A new structure was created in which the Pro-to Leu mutation was created by the edit command of Quanta. This file was subjected to the identical energy minimization procedure as before. The two files (energy-minimized wild type and energy-minimized P732L were superimposed, and structural differences were investigated). Visual inspection revealed small, localized changes, and a full root-mean-square analysis of the structural differences was not considered necessary.

Results

Selection and in Vivo Characterization of mAMSA Resistant Yeast Transformants

To identify mutations in DNA topo IIβ that confer resistance to mAMSA, a forced molecular evolution approach was used. Three plasmids conferred resistance to mAMSA. Two of the plasmids (mAMSA 1 and 13) that supported growth on 10 μg/ml bore the same point change, a C-to-T change at base 1394, resulting in a glycine-to-aspartic acid substitution at amino acid residue 465 (G465D). One transformant, mAMSA 7, was also able to grow on plates containing 200 μg/ml. This most resistant transformant, mAMSA 7, contained the plasmid YEphTOP2βKLM, bearing a transition mutation C→T at position 2195 bp, resulting in a proline-to-leucine amino acid change at residue 732, YEphTOP2βP732L. Here we report the detailed characterization of βP732L.

βP732L Is Resistant to All Antitopoisomerase II Drugs Tested

βP732L was able to complement the endogenous yeast enzyme at 35°C, confirming that this mutated protein is functional in vivo. The level of drug resistance to the selecting agent mAMSA was assessed in 2 ways. It was quantified using the MLC method (Nitiss, 1994). JN394 top2-4 were transformed with plasmid encoding βwt or βP732L and were grown in the presence of different concentrations of mAMSA for 6 and 24 h (Fig. 1, A and B). Figure 1 shows the percentage relative survival versus drug concentration; the drug concentration that gave 100% survival was taken as the MLC. The MLC for βwt transformants on mAMSA was 1.5 μg/ml after 6 h and 2.4 μg/ml after 24 h (Fig. 1, A and B). Yeast transformants expressing βP732L survived at higher mAMSA levels; thus, these transformants were exposed to a higher dose range. The MLC for βP732L transformant on

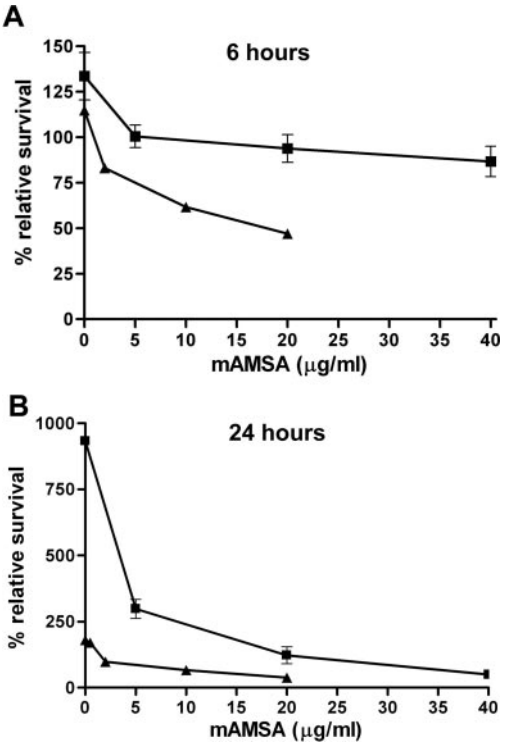

Fig. 1. Effects of mAMSA on the viability of yeast strain JN394 top2-4 transformed with plasmids encoding recombinant βwt or βP732L at 35°C. Viable counts were determined after growth of yeast transformants in the absence or presence of mAMSA at the concentrations indicated for 0, 6, or 24 h. The values are expressed as a percentage of viable counts measured for time 0, percentage of relative survival. The results are the average of three independent experiments. Error bars represent the S.E.M. of three experiments. A shows the 6-h exposure to mAMSA and B shows the 24-h exposure. Plots of JN394 top2-4-expressing βwt (▲) and JN394 top2-4-expressing βP732L (■) are shown.

mAMSA was 14.8 μg/ml after 6 h and 24.8 μg/ml after 24 h (Fig. 1, A and B). Thus, βP732L conferred 9.9-fold resistance to mAMSA compared with the wild type. This difference was found to be statistically significant when a paired, two-tailed *t* test was employed ($p < 0.05$).

Cross-resistance to other drugs was tested qualitatively by continuous exposure to drug (Leontiou et al., 2004). JN394 top2-4 expressing either βwt or βP732L was grown on YPDA plates containing different drugs, including mAMSA, AMCA, mAMCA, etoposide, ellipticine, or doxorubicin. βP732L was found to be resistant to all the drugs tested, ranging between ~2- and ~50-fold (Table 1).

βP732L Shows Decreased Strand Passage Activities Compared with the βwt Protein

Wild-type and mutated proteins were expressed in yeast, and the enzymes were purified to >95% homogeneity (Fig. 2A). Purified βP732L and βwt proteins were assayed for strand passage activity by both decatenation of kDNA and relaxation of supercoiled plasmid DNA. βP732L had significantly reduced relaxation activity (56.5 ± 8.2%) compared with the wild-type protein and reduced in vitro decatenation activity (74.4 ± 29.3%) compared with the wild-type protein (Fig. 2B).

The $MgCl_2$ and ATP dependence of βP732L for decatenation was also measured. Decatenation was carried out in the presence of increasing concentrations of $MgCl_2$. The βwt enzyme showed maximal decatenation activity between 10 and 40 mM $MgCl_2$, whereas βP732L showed a narrower range between 10 and 30 mM $MgCl_2$ for maximal decatenation activity, thus βP732L is slightly more sensitive to increased concentrations of magnesium (Fig. 2C). Analysis of the ATP dependence showed that βP732L did not have an altered ATP requirement for in vitro decatenation of kDNA (Fig. 2D).

βP732L Has Altered DNA Binding Properties Compared with βwt

βwt bound to all three substrates tested (linear, four-way junction, and bent DNA) with comparable affinity, the K_D values were in the range of 1 to 3 nM (Leontiou et al., 2003). For the wild-type protein, the data best fit the simple 1:1 (Langmuir) model for all three substrates. βP732L bound to four-way junction DNA with similar kinetics to βwt, with a K_D of ~1 nM (Fig. 2E). However, unlike the βwt, βP732L binding to the linear and bent DNA substrates did not fit a Langmuir binding model, so no K_D values could be determined for these substrates.

βP732L Protein Has Altered DNA Cleavage Properties Compared with βwt

Cleavage of a 40-bp Oligonucleotide. The ability of the βwt and βP732L proteins to cleave a 40-bp linear DNA substrate was tested (Fig. 3A). This substrate contains one mAMSA site that is cleaved strongly in the presence of mAMSA and weakly in its absence, to produce two cleavage products of 21 and 15 nucleotides (Marsh et al., 1996).

The βwt protein weakly cleaved the DNA substrate in the presence of magnesium ions (7.8 ± 2.4%) (Fig. 3A, lane 2) and addition of mAMSA enhanced the levels of cleavage by 12.8-fold (100%) (Fig. 3A, lane 3). Cleavage in the presence of calcium ions was increased by 5-fold (42 ± 7.7%) (Fig. 3A, lane 4), compared with magnesium alone (7.8 ± 2.4%) (Fig. 3A, lane 2). Cleavage was highest in the presence of calcium and mAMSA (376.4 ± 97.6%) (Fig. 3A, lane 5), approximately 50-fold higher than with magnesium and no drug (Fig. 3A, lane 2), 9-fold higher than calcium alone (Fig. 3A, lane 4), and ~4-fold higher than magnesium plus mAMSA (Fig. 3A, lane 3).

Cleavage of the 40-bp substrate by βP732L was very different from cleavage of this substrate by βwt protein, in the presence of Mg^{2+} ions, it produced a ladder of approximately 15 cleavage products (Fig. 3A, lane 6), not the expected two products of 15 and 21 nucleotides. The amount of cleavage by βP732L with magnesium was greater than βwt under the same conditions (Fig. 3A, lanes 2 and 6). This cleavage by βP732L was not further stimulated by mAMSA (Fig. 3A, lane 7), unlike βwt, the magnesium cleavage of which was stimulated 13-fold by mAMSA. It is striking that βP732L was not able to cleave DNA in the presence of calcium ions (Fig. 3A, lane 8), even when mAMSA was added in the reaction (Fig. 3A lane 9). Cleavage of this 40-bp oligonucleotide by βwt can also be stimulated by etoposide. However, etoposide did not further stimulate cleavage by βP732L on this 40-bp substrate, the cleavage products gave the same pattern and intensity with or without drug (Fig. 3B), indicating that βP732L cleavage of the 40-bp oligonucleotide substrate in the presence of magnesium is not further stimulated by mAMSA or etoposide.

TABLE 1

The drug sensitivity profile of JN394 top2-4 expressing βwt or βP732L in the presence of different cytotoxics at 35°C

The yeast strain JN394 top2–4 was transformed with recombinant plasmid encoding either βwt or βP732L. The transformed strains were tested for drug sensitivity to different concentrations of topo II poisons. Equal amounts of each transformant as determined by optical density were plated in a series of dilutions onto adenie-supplemented yeast extract/peptone/dextrose with drug and were grown at 35°C for 5 days. After 5 days, the extent of growth was assessed by comparing the number of yeast colonies with the wild type. The result shown here is the amount of growth of yeast colonies. Comparisons of the level of growth from several dilutions on plates containing several different drug concentrations allowed approximate -fold resistance values to be determined. The experiment was performed in duplicate.

Drug	Plasmid	1 μg/ml	5 μg/ml	10 μg/ml	25 μg/ml	50 μg/ml	100 μg/ml	200 μg/ml	Resistance
mAMSA	YEphtop2βKLM	+++++	+++	–	–	–	N.D.	N.D.	~10-fold
	YEphtop2βP732L	+++++	+++++	+++	+++	+++	N.D.	N.D.	
mAMCA	YEphtop2βKLM	++++	–	–	–	–	N.D.	N.D.	~50-fold
	YEphtop2βP732L	+++++	+++++	++++	++++	++++	N.D.	N.D.	
AMCA	YEphtop2βKLM	++++	+/–	+/–	–	–	N.D.	N.D.	~10-fold
	YEphtop2βP732L	+++++	+++++	+++++	+++++	+++++	N.D.	N.D.	
Etoposide	YEphtop2βKLM	N.D.	N.D.	++++	++++	++++	+++	++	~2-fold
	YEphtop2βP732L	N.D.	N.D.	+++++	+++++	++++	++++	++++	
Doxorubicin	YEphtop2βKLM	N.D.	++++	++++	+/–	–	N.D.	N.D.	~4-fold
	YEphtop2βP732L	N.D.	+++++	+++++	+++++	+++++	N.D.	N.D.	
Ellipticine	YEphtop2βKLM	N.D.	++++	+++	+	–	–	N.D.	~8-fold
	YEphtop2βP732L	N.D.	+++++	+++++	+++++	+++++	+++++	N.D.	

N.D., not determined; +++++, excellent growth (e.g., good at all dilutions); ++++, very good growth; +++, good growth; ++, reasonable growth; +, poor growth; –, no growth.

Cleavage of a 564-bp Fragment of pBR322. To further investigate the cleavage characteristics of βP732L, a 564-bp fragment of pBR322 was isolated by polymerase chain reaction and end-labeled. βP732L did not produce the same-size cleavage products as the βwt protein. Cleavage of the 564-bp substrate was carried out in the presence of magnesium and mAMSA (Fig. 3C, lanes 2 and 6). Under these conditions, the βP732L protein (Fig. 3C, lane 6), produced different cleavage products compared with βwt with magnesium and mAMSA (Fig. 3C, lane 2). Cleavage of the 564-bp substrate by βP732L was also carried out in the presence of calcium ions and mAMSA; βP732L was unable to support cleavage in the presence of calcium ions (Fig. 3C, lane 7), unlike βwt under these conditions (Fig. 3C, lane 3).

Cleavage with manganese and nickel was analyzed for βwt and βP732L (Fig. 3C, lanes 4, 5, 8, and 9). Manganese and nickel supported cleavage with both βwt and βP732L. The βP732L cleavage with manganese or nickel was more promiscuous than βwt, as seen with magnesium, cleaving in more positions resulting in a different cleavage pattern. βwt cleavage with nickel was less intense than with manganese; this difference was not seen with βP732L.

βP732L Forms More Stable Cleavable Complexes in the Absence or Presence of mAMSA Compared with βwt

The salt reversal of the complexes on the 564-bp substrate was assessed to determine the in vitro stability of the complexes with either βwt or βP732L (Fig. 4). The level of cleav-

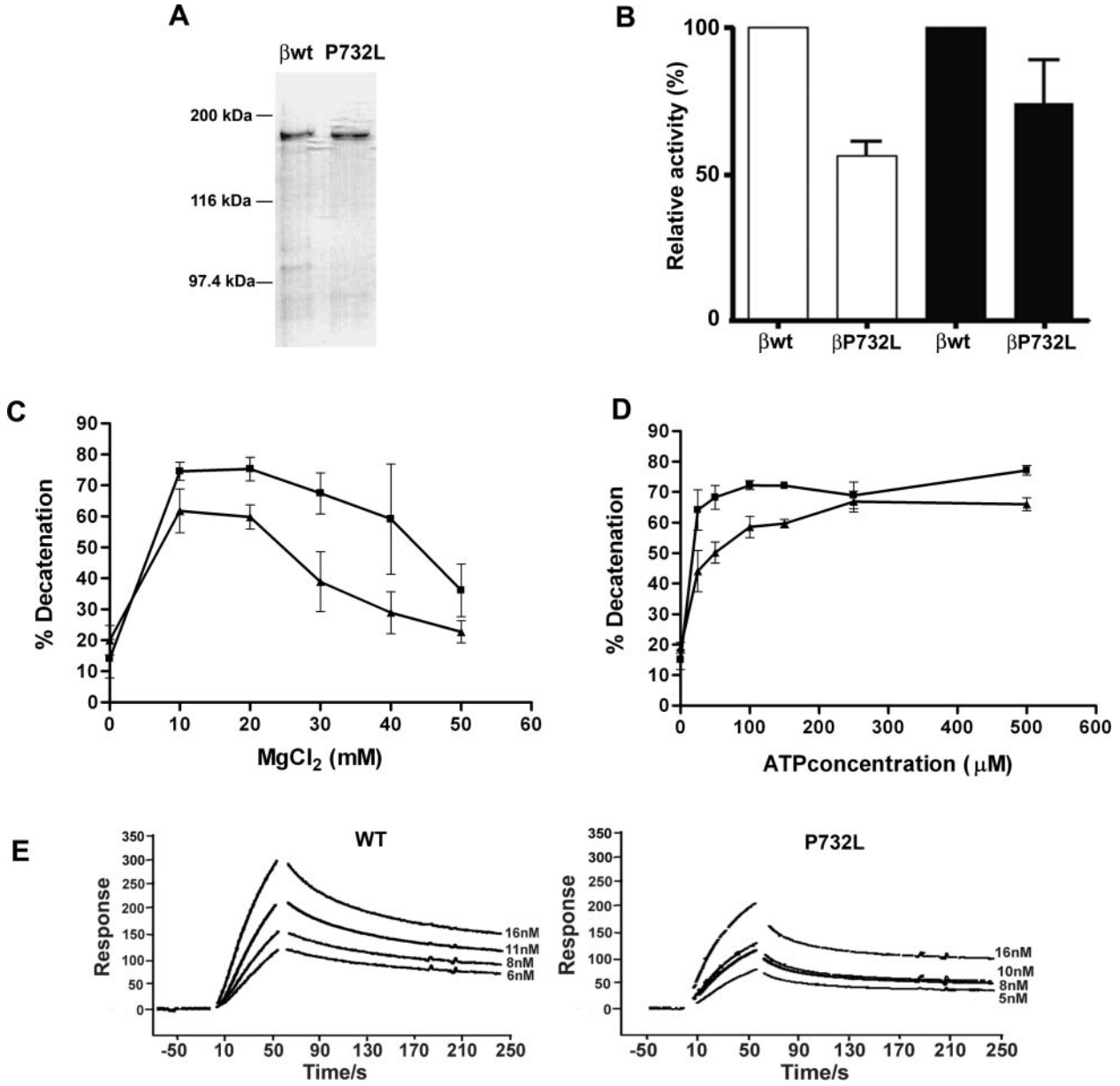

Fig. 2. A, a 7.5% SDS-PAGE gel loaded with 1.5 μg of βwt or βP732L and stained with Coomassie blue. B, strand passage activity, histograms of the relative relaxation activity (□) and relative decatenation (■) for βwt and βP732L. βwt is set to 100%. Means were calculated from at least three experiments; error bars represent 1 S.D. from the mean. C, effect of Mg^{2+} concentration on decatenation by βwt (■) and βP732L (▲). Mean and S.D. are derived from at least three experiments. D, effect of ATP concentration by βwt (■) and βP732L (▲). Mean and S.D. are are derived from at least three experiments. E, DNA binding of human topo II βwt and βP732L by surface plasmon resonance to four-way junction DNA. The experiment was carried out at 25°C, the association phase was 80 s. Resonance units are plotted versus time.

age with βwt with only magnesium was too low to accurately determine the reversal times, but salt reversal of βwt with magnesium and mAMSA is shown in Fig. 4A, the half-lives of complexes were ~5 min, and all the complexes had reversed within 20 min. In contrast, βP732L complexes in the presence of magnesium either with or without mAMSA (Fig. 4, B and C, respectively) were all still present after 20 min, showing that their stability was greater than βwt and this stability was not drug-dependent.

Cleavage of Linearized 4.3-Kilobase Fragment of pBR322. βP732L cleavage of a linearized 4.3-kilobase fragment was tested. With both mAMSA and etoposide, the cleavage pattern resembled βwt in the presence of magnesium (Fig. 5A). On this substrate, no cleavage was seen in the absence of drug (data not shown).

Cleavage of Supercoiled Plasmid Substrate by βwt and βP732L in the Presence of Mg^{2+} or Ca^{2+}. To test whether βP732L was able to cleave longer substrates in the presence of calcium, we tested the magnesium and calcium cleavage of supercoiled plasmid DNA both in the presence and in the absence of mAMSA (Fig. 5B). βwt cleaved weakly with magnesium (Fig. 5B, lane 2) and well with calcium (Fig. 5B, lane 3), and with either magnesium or calcium, mAMSA increases the level of cleavage (Fig. 5B, lanes 4 and 5).

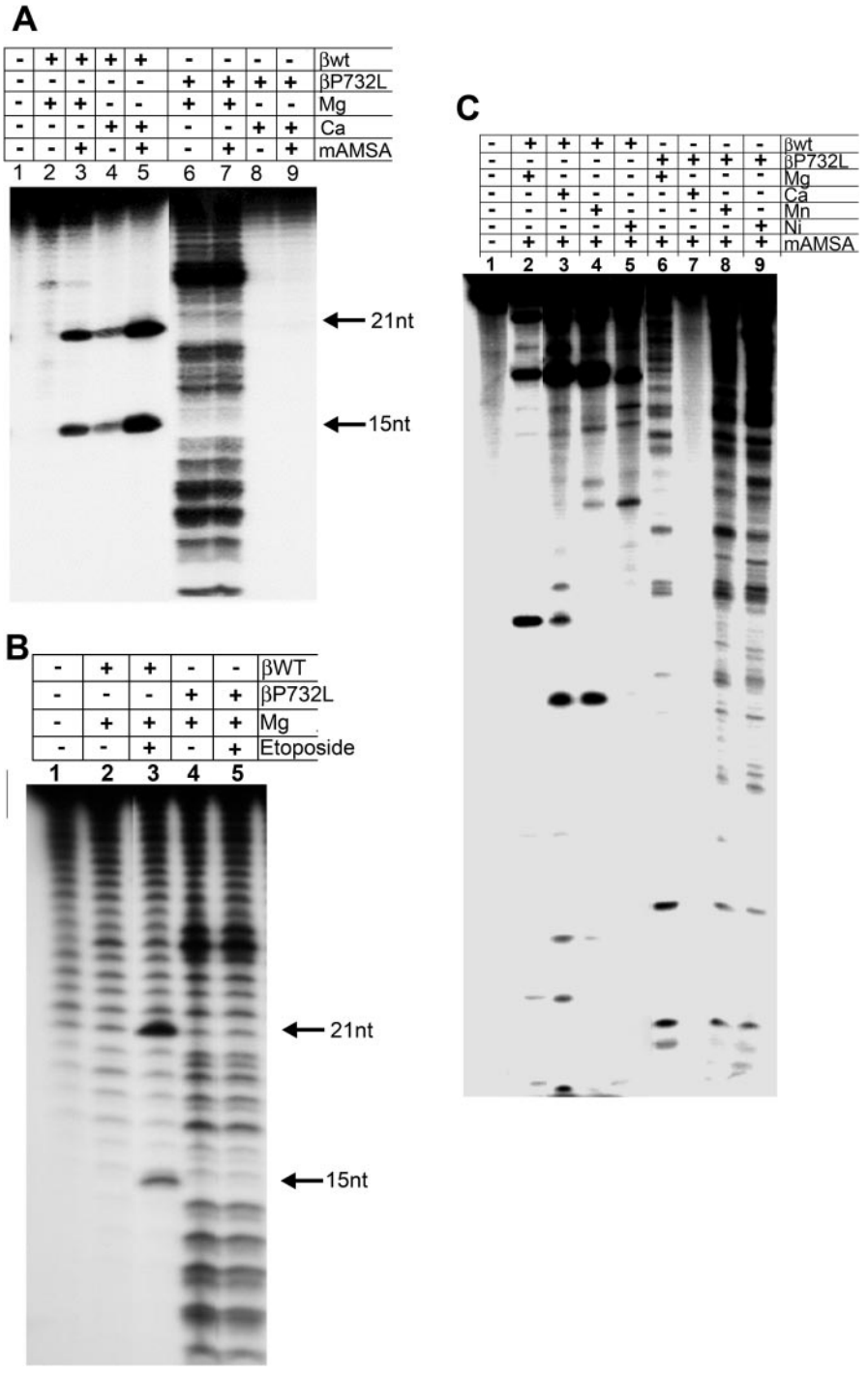

Fig. 3. A, cleavage of the ^{32}P-labeled 40-bp DNA substrate by βwt and βP732L. Cleavage was carried out in the presence of no protein (lane 1) or 1.2 μg of βwt (lanes 2–5) or βP732L (lanes 6–9), plus Mg^{2+} (lanes 2 and 6), Mg^{2+} and mAMSA (lanes 3 and 7), Ca^{2+} (lanes 4 and 8), and Ca^{2+} and mAMSA (lanes 5 and 9). Cleavage products were quantified by filmless autoradiographic analysis using a Fujifilm BAS-1500 machine. This figure shows an individual experiment that is typical of at least three others. B, cleavage of the ^{32}P-labeled 40-bp DNA substrate by βwt and βP732L. Cleavage was carried out in the presence of no protein (lane 1) or 1.2 μg of βwt (lanes 2 and 3) or βP732L (lanes 4 and 5), plus Mg^{2+} (lanes 2 and 4) or Mg^{2+} and etoposide (lanes 3 and 5). Cleavage products were quantified by filmless autoradiographic analysis using a Fujifilm BAS-1500 machine. C, cleavage of the ^{32}P-labeled 564-bp DNA substrate by βwt and βP732L. Protein (1.2 μg) was incubated with the 564-bp ^{32}P-labeled pBR322 substrate for 30 min at 37°C in the presence of various cations and mAMSA and either βwt (lanes 2–5) or β732L (lanes 6–9). Lane 1, no protein; lanes 2 and 6, Mg^{2+} + mAMSA; lanes 3 and 7, Ca^{2+} + mAMSA; lanes 4 and 8, Mn^{2+} + mAMSA; lanes 5 and 9, Ni^{2+} + mAMSA.

βP732L showed more cleavage than βwt with magnesium alone (Fig. 5B, lanes 6 and 2, respectively). No cleavage was seen with βP732L and calcium (Fig. 5B, lanes 8 and 9), in agreement with the experiments on the 40- and 564-bp linear substrates.

Modeling of the Central Breakage Domains of Wild-Type topo IIβ and βP732L. Type II topoisomerases have three structural domains: an N-terminal ATPase, a central breakage-rejoining domain composed of the A′ and B′ subfragments, and a C-terminal domain (Austin et al., 1995). Residue 732 lies in the A′ subfragment, which spans residues 722 to ~1200 in human topo IIβ. The A′ subfragment can be further subdivided into three sections. The first section of A′ spans residues β722–858 and is termed the "CAP-like" domain as it contains a fold similar to one found in the catabolite activator protein and histone H5 (Berger et al., 1996). This portion of the A′ subfragment also contains the active site tyrosine (Tyr820) responsible for forming the phosphotyrosine linkage with DNA. Pro732 lies at the end of the A′ α1 helix within the CAP-like fold. An alignment of the "*CAP-like*" domain from human topo IIβ, human topo IIα, yeast topo II, and *Escherichia coli* gyrase A (Fig. 6a) shows that this region is conserved between species. Pro732 is a highly conserved residue; a proline is found at the position equivalent to 732 in type II topoisomerases from bacteria to humans.

The sequence similarity between the central breakage and rejoining domain of human topo IIβ and Yeast topo II enabled us to model the human topo IIβ sequence onto the yeast structure (Berger et al., 1996; West et al., 2000). Residues 420 to 1063 of htopo IIβ monomer were modeled onto the yeast crystal structure (EC 5.99.1.3; primary accession number P06786). The computer program Modeler was used, which is conservative in that modeled structures are based very closely on the template structure (Sali and Blundell, 1993). The mutation P732L was then created in the htopo IIβ model to estimate the structural effects of the mutation. Local conformation changes are predicted (Fig. 6, B and D). The leucine residue at 732 adopts an altered position to the proline 732 in the modeled structure, and the peptide backbone is shifted in the vicinity of 732 in the model of the

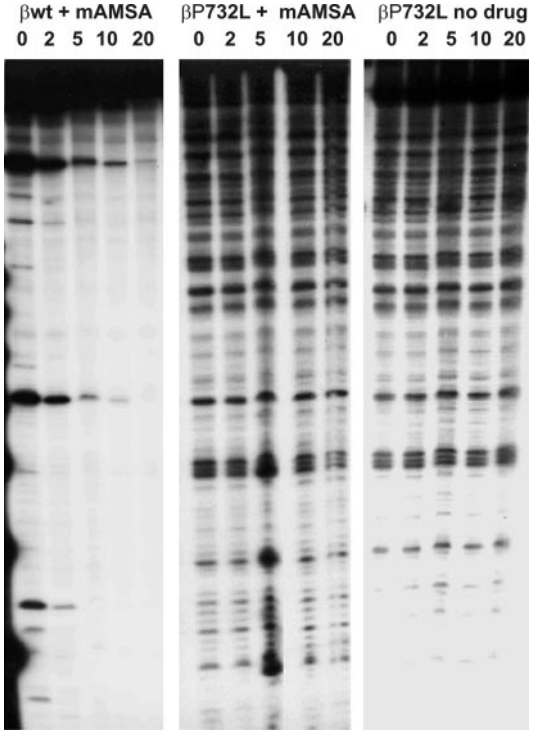

Fig. 4. An autoradiograph of a 564-bp ^{32}P-labeled pBR322 DNA substrate after incubation with or without mAMSA, in the presence of 10 nM $MgCl_2$ and the indicated protein. Reactions were terminated at the noted time points (0–20 min).

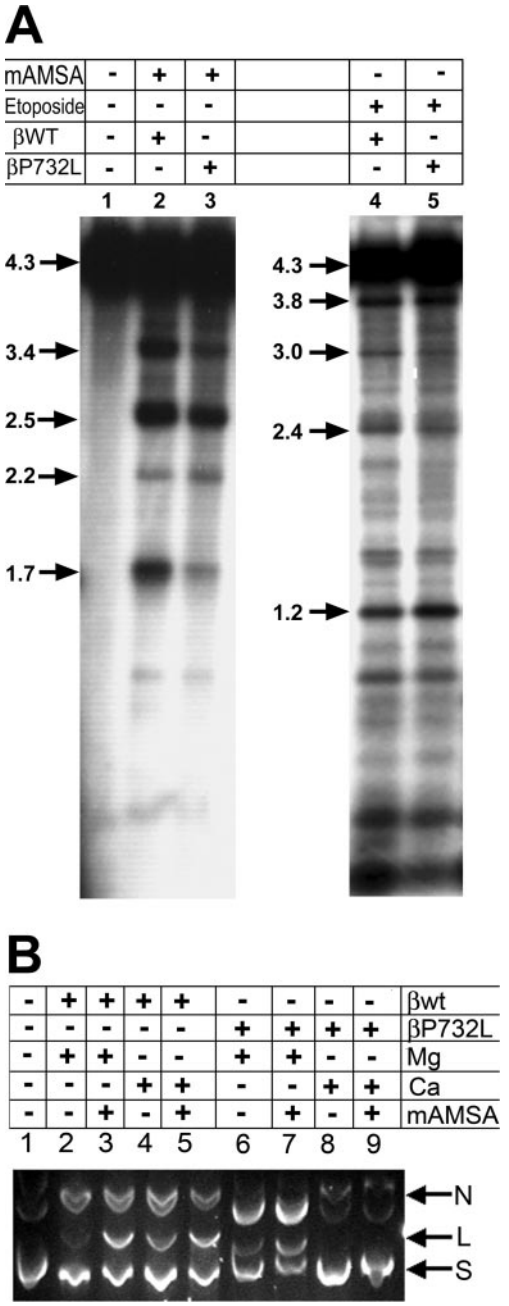

Fig. 5. A, cleavage of the ^{32}P-labeled 4.3-kb pBR322 probe in the presence of mAMSA or etoposide. Lane 1, no protein; lanes 2 and 4, βwt; lanes 3 and 5, βP732L; lanes 2 and 3, with mAMSA; lanes 4 and 5, with etopooside. B, cleavage of supercoiled plasmid DNA by βwt and βP732L. Protein (4 μg) was incubated with 1.5 μg of supercoiled plasmid DNA in relaxation buffer with 10 mM $MgCl_2$ or $CaCl_2$± mAMSA with either βwt (lanes 2–5) or βP732L (lanes 6–9) for 30 min at 37°C. Control supercoiled plasmid (lane 1). Lanes 2 and 6, Mg^{2+}; lanes 3 and 7, Mg^{2+} + mAMSA; lanes 4 and 8, Ca^{2+}; lanes 5 and 10, Ca^{2+} + mAMSA.

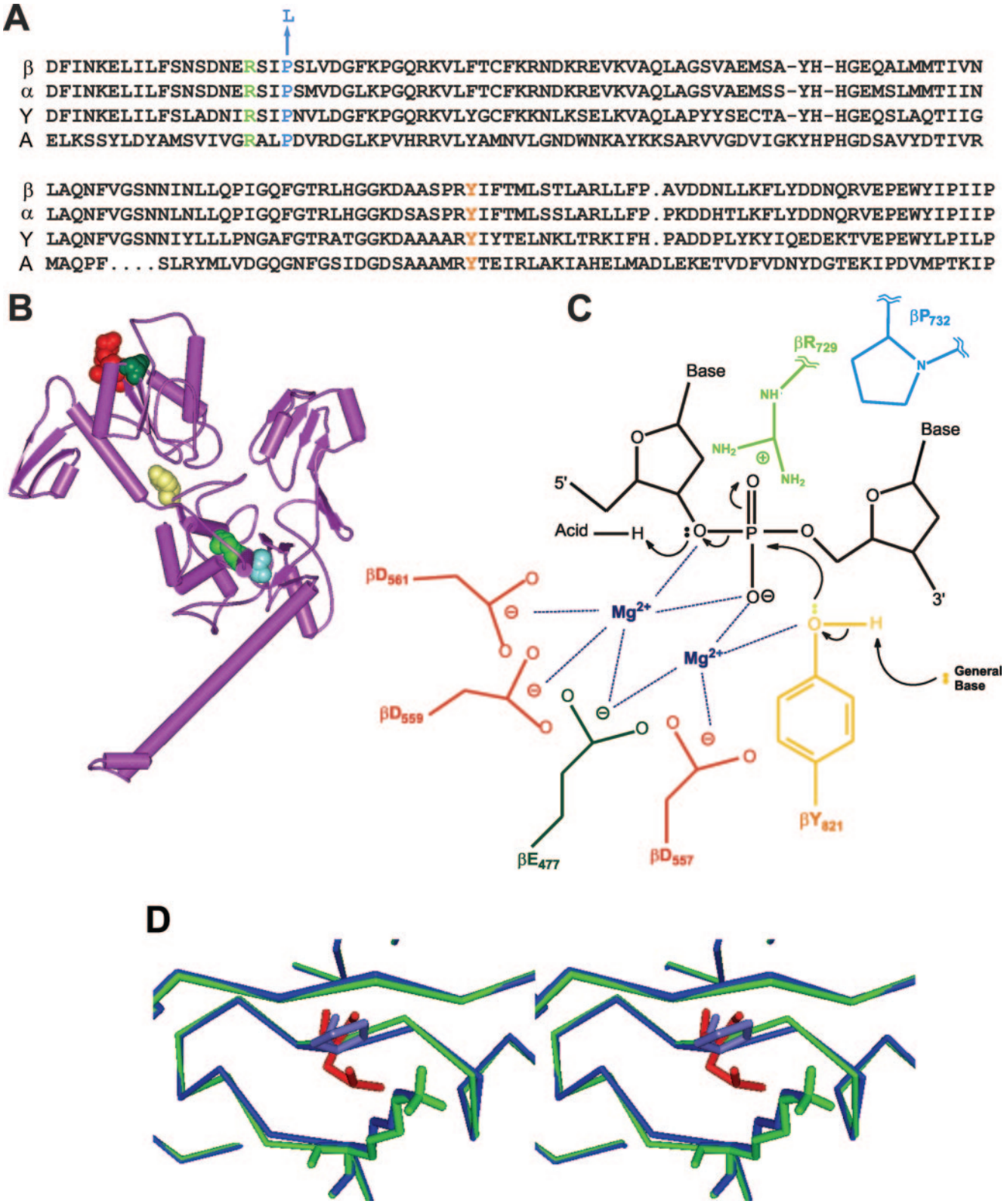

Fig. 6. A, alignment of the "CAP"-like region of human topo IIβ (β) compared with that from human topo IIα (α), yeast topo II (Y), and DNA gyrase A (A). The proline equivalent to Pro732 is shown in light blue, the arginine equivalent to Arg729 is shown in green, and the active site tyrosine is shown in yellow. B, a diagram of one monomer of human topo IIβ showing the location of the P732L mutation in pale blue, the active site tyrosine in yellow, and Arg729 in light green. The location of acidic residues involved in metal ion co-ordination is also shaded. The **E**GDSA motif containing Glu477 is shown in dark green and the IMT**D**Q**D**(Q/H)**D**GSH loop, containing Asp557, Asp559, and Asp561 is shown in red. C, schematic adapted from a model previously proposed by Noble and Maxwell (2002). This shows a two-metal-ion mechanism for the phosphoryl transfer reaction involved in DNA cleavage by DNA topo II. The coloring is equivalent to that seen in A and B. D, a stereo image of the region immediately surrounding residue 732; the wild-type sequence is shown in blue. The mutant chain is green with the leucine side chain shown in red, above which the wild-type proline ring can be seen. The residue numbering is that of human topoisomerase II β-1, which is a 1621-residue protein, not human topoisomerase II β-2, which is a 1626-residue protein (Q02880).

mutated protein (Fig. 6D). Thus, the proline-to-leucine amino acid change at position 732 in the model is not predicted to have any large effects on the overall structure. This is consistent with small, <2-Å alterations in backbone positions and similar alterations in some side chains, (e.g., Lys739). In the model, some new H-bonds are formed (e.g., lysine 739 γ-nitrogen to the backbone at residue 731) because of shifting of the backbone in this region. However, these all rely on the small changes being accurate to better than 1 Å, which is beyond the resolution of the original X-ray structure. The predicted small changes are consistent with the fact that the selection procedure used will only select functional enzymes; amino acid changes that result in large structural changes that inactivate the enzyme would not be isolated.

Discussion

Mutation βP732L confers in vivo drug resistance of ~10-fold to mAMSA in an MLC assay and was cross-resistant to all the topo II drugs tested, including AMCA, mAMCA, etoposide, ellipticine, and doxorubicin (Fig. 1 and Table 1). βP732L is functional in vivo, as our selection screen is dependent upon complementation in yeast. Although βP732L was functional in vivo, its in vitro strand passage activity is reduced compared with the wild type. Binding of βP732L to linear DNA substrates was altered, but binding to a four-way junction substrate was similar to the wild-type enzyme (Fig. 2E).

Our in vitro experimental data with βP732L protein indicates that it has altered cleavage properties. Most striking is that calcium could not support cleavage by βP732L, unlike βwt. Cleavage by βP732L of a 40- or 564-bp linear substrate showed the same differences: greater cleavage with magnesium alone, no drug enhancement, and no cleavage with calcium. On the 40- and 564-bp substrates, cleavage occurred at more sites compared with the βwt enzyme (Fig. 3, A–C, and Fig. 4). However, on the 4.3-kb linearized pBR322, the cleavage pattern appeared similar to βwt (Fig. 5A). This suggests that the altered DNA binding seen on 40- and 189-bp bent DNA substrates may be affecting cleavage site specificity on the shorter DNA substrates. Cleavage reactions using supercoiled plasmid substrate confirmed that calcium did not support cleavage by βP732L on the full-length plasmid, but magnesium did. Using the 564-bp substrate, the cleavage products generated by βP732L were shown to be more stable than those with βwt. This suggests an alteration of the cleavage-religation equilibrium of βP732L, favoring cleavage over religation, producing longer-lived cleavable complexes compared with βwt. This could account for the increase in cleavage products with magnesium in the absence of drug.

Why does this proline-to-leucine change generate a protein whose DNA cleavage reaction cannot be supported by calcium and has an altered cleavage-religation equilibria? To address this question, the position of Pro732 within the protein was analyzed by modeling this region onto the yeast structure. Modeling suggested that the leucine change caused the local peptide backbone in βP732L to shift position compared with βwt. Topoisomerase, however, is a very dynamic protein, and the removal of a highly conserved proline may alter the local mobility during catalysis. This cannot be accurately modeled using the currently available crystal structures of parts of the yeast protein.

A number of residues in this region have previously been demonstrated to be important for enzyme catalysis. Site-directed mutations have been made in this region of the yeast topoisomerase II (Liu and Wang, 1998). Alanine substitutions at yeast Arg690, Asp697, Lys700, Arg704, or Arg781 abolished in vivo function in a complementation assay. The equivalent residues in htopo IIβ are βArg729, βAsp736, βLys739, βArg743, and βArg820, four of which are very close to Pro732.

In the yeast protein, mutating Arg690 to alanine completely abolished in vitro cleavage activity (Liu and Wang, 1998). Yeast arginine 690 is equivalent to Arg32 in Gyrase A. Noble and Maxwell (2002) suggest that this arginine is actively involved in the phosphoryl transfer mechanism that enables topo II to cleave the DNA. The equivalent residue in htopo IIβ is Arg729, which is only three residues away from βPro732, so local conformational changes in the P732L protein may affect the proposed role of this arginine in DNA cleavage.

Phosphoryltransfer reactions have been proposed to involve two metal ions in their mechanism (Beese and Steitz, 1991). The proposed metal binding sites have magnesium ions coordinated by acidic amino acid residues such as aspartic acid and glutamic acid (West et al., 2000). We proposed two potential metal ion binding sites in htopo IIβ coordinated to the aspartic acids found in the IMTDQD(Q/H)DGSH loop, Asp557, Asp559 and Asp561 (West et al., 2000). A similar acidic triad is also found in topoisomerase I, and mutation of these residues reduces the number of magnesium ions bound per protein molecule (Lima et al., 1994; Zhu and Tse-Dinh, 2000). Noble and Maxwell (2002) have published a model for the phosphoryl transfer in DNA cleavage by DNA gyrase. In Fig. 6C, we have adapted the Noble and Maxwell schematic diagram to represent human topo IIβ. βArg729 is shown in light green in Fig. 6C and illustrates the proximity of residue 732 to the hypothesized location of the DNA, active site tyrosine, and the two metal binding sites hypothesized to catalyze the DNA cleavage reaction. The predicted local conformational changes may account for the altered DNA binding to linear DNA observed by SPR. It also suggests an explanation for the cleavage in the presence of magnesium but not calcium ions. If the local conformational change alters the liganding geometry for the bound metal ions, such that calcium can no longer support the phosphoryl transfer reaction and the magnesium supported phosphoryl transfer reaction has an altered equilibrium favoring cleavage over religation, this could account for the greater stability of the cleavage complexes with magnesium and the lack thereof with calcium.

The presence of a contaminating nuclease would offer a simple explanation for the altered cleavage properties with magnesium, such as the extensive cleavage with magnesium alone and the lack of drug stimulation of cleavage in the presence of magnesium on short DNA substrates and lack of reversibility. This possibility is very difficult to exclude because the amounts of such a protein could be so low that polyacrylamide gel electrophoresis or matrix-assisted laser desorption ionization approaches would not be guaranteed to pick it up. However, we do not see this non–drug-stimulated cleavage activity with magnesium in βwt or in four other

mutated proteins expressed using the same system and purified by the same protocol. In addition, we do not see any DNA products that seem to be caused by nuclease activity in any of the agarose gels used for activity assays.

A study in HL-60 cells indicated that an intracellular calcium buffer could reduce the DNA cleavage by topoisomerase II in the presence of either etoposide or mAMSA. This reduction correlated with decreased cytotoxicity (Aoyama et al., 1998). The absence of cleavage with calcium may account for the drug resistance seen in yeast with P732L. However, whether removal of calcium-stimulated cleavage is an important mechanism of drug resistance in human tumors remains to be determined.

Acknowledgments

We thank M. Bell for technical assistance and I. G. Cowell for assistance with the figures.

References

Aoyama M, Grabowski DR, Dubyak GR, Constantinou AI, Rybicki A, Bukowski RM, Ganapathi MK, Hickson ID, and Ganapathi R (1998) Attenuation of drug-stimulated topoisomerase II–DNA cleavable complex formation in wild-type HL-60 cells treated with an intracellular calcium buffer is correlated with decreased cytotoxicity and site-specific hypophosphorylation of topoisomerase IIα. *Biochem J* **336:**727–733.

Austin CA, Marsh KL, Wasserman RA, Willmore E, Sayer PJ, Wang JC, and Fisher LM (1995) Expression, domain structure and enzymatic properties of an active recombinant human DNA topoisomerase II beta. *J Biol Chem* **270:**15739–15746.

Bakic M, Beran M, Andersson BS, Silberman L, Estey E, and Zwelling LA (1986) The production of topoisomerase II-mediated DNA cleavage in human leukemia cells predicts their susceptibility to 4′-(9-acridinylamino)methanesulfon-m-anisidide (m-AMSA). *Biochem Biophys Res Commun* **134:**638–645.

Beese LS and Steitz TA (1991) Structural basis for the 3′-5′ exonuclease activity of Escherichia coli DNA polymerase I: a two metal ion mechanism. *EMBO (Eur Mol Biol Organ) J* **10:**25–33.

Berger JM, Gamblin SJ, Harrison SC, and Wang JC (1996) Structure and mechanism of DNA topoisomerase II. *Nature (Lond)* **379:**225–232.

Dereuddre S, Delaporte C, and Jacquemin-Sablon A (1997) Role of topoisomerase II beta in the resistance of 9-OH-ellipticine-resistant Chinese hamster fibroblasts to topoisomerase II inhibitors. *Cancer Res* **57:**4301–4308.

Errington F, Willmore E, Tilby MJ, Li L, Li G, Li W, Baguley BC, and Austin CA (1999) Murine transgenic cells lacking DNA topoisomerase IIβ are resistant to acridines and mitoxantrone: analysis of cytotoxicity and cleavable complex formation. *Mol Pharmacol* **56:**1309–1316.

Freudenreich CH, Chang C, and Kreuzer KN (1998) Mutations of the bacteriophage T4 type II DNA topoisomerase that alter sensitivity to antitumor agent 4′-(9-acridinylamino)methanesulfon-m-anisidide and an antibacterial quinolone. *Cancer Res* **58:**1260–1267.

Hinds M, Deisseroth K, Mayes J, Altschuler E, Jansen R, Ledley FD, and Zwelling LA (1991) Identification of a point mutation in the topoisomerase II gene from a human leukemia cell line containing an amsacrine-resistant form of topoisomerase II. *Cancer Res* **51:**4729–4731.

Kubo A, Yoshikawa A, Hirashima T, Masuda N, Takada M, Takahara J, Fukuoka M, and Nakagawa K (1996) Point mutations of the topoisomerase IIalpha gene in patients with small cell lung cancer treated with etoposide. *Cancer Res* **56:**1232–1236.

Lee MS, Wang JC, and Beran M (1992) Two independent amsacrine-resistant human myeloid leukemia cell lines share an identical point mutation in the 170 kDa form of human topoisomerase II. *J Mol Biol* **223:**837–843.

Leontiou C, Lakey JH, and Austin CA (2004) Mutation E522K in human DNA topoisomerase IIbeta confers resistance to methyl N-(4′-(9-acridinylamino)-phenyl)carbamate hydrochloride and methyl N-(4′-(9-acridinylamino)-3-methoxyphenyl) methane sulfonamide but hypersensitivity to etoposide. *Mol Pharmacol* **66:**430–439.

Leontiou C, Lightowlers RN, Lakey JH, and Austin CA (2003) Kinetic analysis of human topoisomerase IIalpha and beta DNA binding by surface plasmon resonance. *FEBS Lett* **554:**206–210.

Lima CD, Wang JC, and Mondragon A (1994) Three-dimensional structure of the 67K N-terminal fragment of E. coli DNA topoisomerase I. *Nature (Lond)* **367:**138–146.

Liu Q and Wang JC (1998) Identification of active site residues in the "GyrA" half of yeast DNA topoisomerase II. *J Biol Chem* **273:**20252–20260.

Marsh KL, Willmore E, Tinelli S, Cornarotti M, Meczes EL, Capranico G, Fisher LM, and Austin CA (1996) Amsacrine-promoted DNA cleavage site determinants for the two human DNA topoisomerase II isoforms alpha and beta. *Biochem Pharmacol* **52:**1675–1685.

Meczes EL, Marsh KL, Fisher LM, Rogers MP, and Austin CA (1997) Complementation of temperature-sensitive topoisomerase II mutations in *Saccharomyces cerevisiae* by a human TOP2 beta construct allows the study of topoisomerase II beta inhibitors in yeast. *Cancer Chemother Pharmacol* **39:**367–375.

Nitiss JL (1994) Using yeast to study resistance to topoisomerase II-targeting drugs. *Cancer Chemother Pharmacol* **34 (Suppl):**S6–S13.

Noble CG and Maxwell A (2002) The role of GyrB in the DNA cleavage-religation reaction of DNA gyrase: a proposed two metal-ion mechanism. *J Mol Biol* **318:**361–371.

Osheroff N and Zechiedrich EL (1987) Calcium-promoted DNA cleavage by eukaryotic topoisomerase II: trapping the covalent enzyme-DNA complex in an active form. *Biochemistry* **26:**4303–4309.

Patel S, Keller BA, and Fisher LM (2000) Mutations at Arg486 and Glu571 in human topoisomerase IIα confer resistance to amsacrine: relevance for antitumor drug resistance in human cells. *Mol Pharmacol* **57:**784–791.

Pommier Y (1993) DNA topoisomerase I and II in cancer chemotherapy: update and perspectives. *Cancer Chemother Pharmacol* **32:**103–108.

Pommier Y, Capranico G, Orr A, and Kohn KW (1991) Local base sequence preferences for DNA cleavage by mammalian topoisomerase II in the presence of amsacrine or teniposide. *Nucleic Acids Res* **19:**5973–5980.

Robinson MJ and Osheroff N (1991) Effects of antineoplastic drugs on the post-strand-passage DNA cleavage/religation equilibrium of topoisomerase II. *Biochemistry* **30:**1807–1813.

Sali A and Blundell TL (1993) Comparative protein modelling by satisfaction of spatial restraints. *J Mol Biol* **234:**779–815.

Tewey KM, Chen GL, Nelson EM, and Liu LF (1984) Intercalative antitumor drugs interfere with the breakage-reunion reaction of mammalian DNA topoisomerase II. *J Biol Chem* **259:**9182–9187.

Wang JC (2002) Cellular roles of DNA topoisomerases: a molecular perspective. *Nat Rev Mol Cell Biol* **3:**430–440.

Wasserman RA and Wang JC (1994) Analysis of yeast DNA topoisomerase II mutants resistant to the antitumor drug amsacrine. *Cancer Res* **54:**1795–1800.

West KL, Meczes EL, Thorn R, Turnbull RM, Marshall R, and Austin CA (2000) Mutagenesis of E477 or K505 in the B′ domain of human topoisomerase II beta increases the requirement for magnesium ions during strand passage. *Biochemistry* **39:**1223–1233.

Zhu CX and Tse-Dinh YC (2000) The acidic triad conserved in type IA DNA topoisomerases is required for binding of Mg(II) and subsequent conformational change. *J Biol Chem* **275:**5318–5322.

Address correspondence to: Professor Caroline A. Austin, Lab 3011, Institute for Cell and Molecular Bioscience, The Medical School, University of Newcastle, Newcastle upon Tyne, NE2 4HH, UK. E-mail: caroline.austin@ncl.ac.uk